Direct perturbation of lens membrane structure may contribute to cataracts caused by U18666A, an oxidosqualene cyclase inhibitor

Richard J. Cenedella,[1,*] Robert Jacob,[†] Douglas Borchman,[§] Daxin Tang,[§] Amanda R. Neely,[*] Abbas Samadi,[*] R. Preston Mason,[†] and Patricia Sexton[*]

Department of Biochemistry,* Kirksville College of Osteopathic Medicine, Kirksville, MO 63501; Elucida Research,† Beverly, MA 01915; and Department of Ophthalmology and Visual Science,§ University of Louisville, Louisville, KY 40202

Abstract Induction of cataracts in experimental animals is a common toxic feature of oxidosqualene cyclase (OSC) inhibitors. U18666A has been shown to produce irreversible lens damage within a few weeks of treatment. Drug actions, besides reducing the availability of cholesterol, could contribute to cataract formation. Cholesterol added to cultures of lens epithelial cells could only partially overcome the growth-inhibiting effects of U18666A. In view of this finding and the fact that U18666A and other OSC inhibitors are highly lipophilic cationic tertiary amines, we tested the hypothesis that the cataractogenic effect of U18666A is related to direct perturbation of lens membrane structure and function. Based on changes in the anisotropy of fluorescent probes, U18666A incorporated into bovine lens lipid model membranes increased membrane structural order and, using small-angle x-ray diffraction, U18666A was shown to intercalate into the lens lipid model membranes and produce a broad condensing effect on membrane structure. Also, exposure of cultured lens epithelial cells and intact rat lenses to U18666A induced apoptosis. Induction of apoptosis may begin by intercalation of U18666A into cell membranes. By increasing membrane structural order, U18666A may also increase light scatter, thus directly contributing to lens opacification.—Cenedella, R. J., R. Jacob, D. Borchman, D. Tang, A. R. Neely, A. Samadi, R. P. Mason, and P. Sexton. **Direct perturbation of lens membrane structure may contribute to cataracts caused by U18666A, an oxidosqualene cyclase inhibitor. *J. Lipid Res.* 2004.** 45: **1232–1241.**

Supplementary key words cholesterol • lens membrane lipids • anisotropy • x-ray diffraction • apoptosis

Blocking key steps in the cholesterol biosynthetic pathway in the ocular lens, by either genetic defect or pharmacological intervention, increases the risk of cataracts in humans and experimental animals (1). Genetically based deficiencies in mevalonate kinase (2), Δ8,Δ7-sterol isomerase (emapomil binding protein) (3), 3β-hydroxysterol Δ7-reductase (4), and 3β-hydroxysterol Δ24-reductase (5) can result in human cataracts. Pharmacological inhibition of desmosterol reductase (6) or oxidosqualene cyclase (OSC) (7, 8) causes cataracts in rodents, and inhibition of HMG-CoA reductase by statins can induce cataracts in rats (9) and increase the risk of cataracts in humans (10). Simvastatin was shown to cause rapid lens damage and induce the formation of cataracts in Chbb:Thom rats (9). Simvastatin treatment also tripled the risk of cataracts in humans who concomitantly received two or more courses of erythromycin (10). Erythromycin can block statin catabolism and greatly increase its blood levels (11).

Pharmaceutical companies have been exploring the development of a new generation of hypocholesterolemic drugs that inhibit the OSC-catalyzed step in the cholesterol biosynthetic pathway (8, 12–15). The potential advantages over the statins, collectively the most prescribed drugs in the United States, include less secondary increase of HMG-CoA reductase and uninhibited formation of isoprenes, intermediates that are formed in the cholesterol pathway between mevalonic acid and squalene and that are essential for cell function (**Fig. 1**). One disadvantage of these drugs, however, is that they may be more cataractogenic than the statins. OSC inhibitors can rapidly induce cataracts in rodents, suggesting that the procataractogenic effects of these drugs may be attributable to mechanisms unrelated to the inhibition of cholesterol biosynthesis. OSC inhibitors constitute a class of amphiphilic, cationic-tertiary amines that include U18666A from Upjohn (now Pharmacia-Upjohn) (12), BIBX79 and BIBB 515 from

Manuscript received 12 November 2003, in revised form 1 March 2004, and in re-revised form 20 April 2004.

Published, JLR Papers in Press, April 21, 2004.
DOI 10.1194/jlr.M300469-JLR200

[1] To whom correspondence should be addressed.
e-mail: rcenedella@kcom.edu

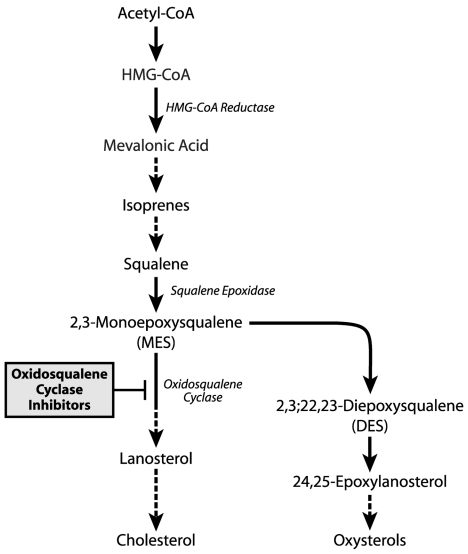

Fig. 1. Inhibition of the sterol synthesis pathway by oxidosqualene cyclase (OSC) inhibitors. Modified from Mark, M., P. Muller, R. Maier, and B. Eisele. 1996. Effects of a novel 2,3-oxidosqualene cyclase inhibitor on the regulation of cholesterol biosynthesis in HepG2 cells. *J. Lipid Res.* **37:** 148–158, with permission of the publisher.

Boehringer Ingelheim (13, 14), Ro48-8071 from Hoffmann-La Roche (15), and ZD9720 and ZD7851 from AstraZeneca (8). U18666A (7), ZD9720 (8), ZD7851 (8), Ro48-8071, and Ro61-0842 can induce cataracts in rats, mice, and dogs after only 10–20 days of treatment. The possibility that these compounds induce cataracts by actions independent of inhibiting cholesterol biosynthesis is suggested by at least two observations. First, the phenothiazide antipsychotic drugs are also cationic-tertiary amines that have no known effects on cholesterol synthesis, yet they are reported to increase the risk of cataracts in treated patients (16). Second, the rapidity with which ZD9720 and ZD7851 induced cataracts in grown dogs and mice (8) suggests that these drugs had a more direct mechanism of toxicity (the cholesterol content of the lens would not be expected to decrease in such a short time). Based on these findings, we hypothesized that the procataractogenic effects may involve direct perturbation of lens membrane structure, because amphiphilic molecules such as propranolol (17) and various steroid hormones (18) are known to intercalate into cell membranes, altering their structure and function.

In the present study, we examine the capacity of U18666A to induce rapid direct effects on lens and lens cells. U18666A is the most broadly studied OSC inhibitor (1). The capacity of U18666A to alter membrane order or fluidity was assessed by measuring changes in the anisotropy of probes that partition to specific membrane regions or domains. Small-angle X-ray-scattering approaches were used to measure the time-averaged membrane location of U18666A as well as the direct effects of this drug on model and native lens lipid membrane structure. We also considered the possibility that the U18666A-induced cataract may be attributable to the induction of apoptosis in lens epithelial cells.

EXPERIMENTAL PROCEDURES

Cataract formation

Twenty day old Sprague-Dawley rats (Hilltop Lab Animals, Scottdale, PA) were fed compressed-ground Purina rat chow containing no inhibitor (controls) or 0.035% U18666A (350 mg drug/kg chow), 0.10% Ro48-8071, or 0.10% Ro61-0842. Estimating that the rats consume ~100 g of chow per kilogram of body weight per day, these levels roughly equate to 35 and 100 mg inhibitor/kg/day. Rats were treated for up to 50 days. Rats were killed by carbon dioxide inhalation. When lens lipids were to be measured, rats were killed 2–3 days after the first appearance of cataracts. Age-matched controls were also killed. Lenses were excised, total lipids were extracted, and sterols and phospholipids were quantitated as done before (19).

Cell and lens culture

J774 mouse macrophages were obtained from the American Type Culture Collection (ATCC; Manassas, VA) and cultured in DMEM containing 10% fetal bovine serum as recommended by the ATCC protocol. Bovine lens epithelial cells (BLECs) were cultured in DMEM containing 10% (w/w) whole calf serum (WCS) or lipid-deficient calf serum (LDCS) (20) as previously prepared (21). Bovine eyes from cattle slaughtered for human food were placed on ice and used within a few hours of slaughter. Twenty-four hours after seeding cells at 50,000 per well (24-well culture dishes) in DMEM + 10% WCS, cells in three wells were counted to establish a zero-time cell density. Cell layers were then washed in serum-free DMEM, and the medium was replaced with DMEM + 10% LDCS containing no inhibitor (controls) or OSC inhibitor, U18666A. U18666A was added in 1.5 μl of ethanol per milliliter of medium. Control medium contained an equal volume of ethanol. Cell numbers in each well were measured 48 h later. In some cases, the medium was replaced to contain 10% WCS supplemented with 50 μg/ml cholesterol with or without U18666A (30 or 200 nM). WCS alone contains ~1.3 mg cholesterol/ml. The effects of U18666A on the apoptosis of BLEC and J774 macrophages cultured in medium with whole serum were assessed at various times after drug addition using the DeadEnd Colorimetric Apoptosis Detection System (Promega, Madison, WI) essentially as recently described (9). Using this technique, we additionally examined the capacity of U18666A to induce apoptosis in the epithelial cell layer of intact rat lenses incubated with U18666A and in lenses of rats treated for 2–4 weeks with U18666A (0.035% in chow). Intact lenses from 22–30 day old Sprague-Dawley rats were organ cultured for up to 2 days in TC199 medium as done before (9) containing 0–400 nM U18666A.

Measurement of lens epithelial cell sterol synthesis in vitro

A concentration of U18666A estimated to completely arrest BLEC growth was tested for the capacity to inhibit cholesterol synthesis from [^{14}C]acetate. Near confluent to confluent dishes of BLECs (third day of subculture) were washed twice in serum-free DMEM and incubated for 4 h at 37°C (95% O_2 and 5% CO_2) in 2.5 ml of DMEM + 10% LDCS containing 8.2 μCi of [1-^{14}C]sodium acetate (55 μCi/μmol; New England Nuclear Corp.) and no inhibitor (control) or 40 nM U18666A. Cell layers of individual dishes were dissolved in 1 ml of 1 N KOH in 50% ethanol; aliquots were taken for protein assay and the remainder were saponified for 1 h at 100°C. Labeled sterols were recovered, and the ^{14}C content was measured as recently described (9).

Anisotropic measurements

Preparation of lipid vesicles. A monophasic extraction procedure performed under argon gas was used to recover total lipids from

whole bovine lenses (22). Individual lenses were homogenized in methanol (5 ml) and sonicated three to four times for 15 s. After centrifugation (5,000 rpm for 1 h), the supernatant was recovered and evaporated under argon. Multilaminar vesicles were prepared from the lens total lipids and from a model phospholipid [1-palmitoyl-2-oleoyl-*sn*-glycerol-3-phosphotidylcholine (POPC)] by vortexing in buffer. Vesicles containing U18666A were prepared at 2.91 mol% in POPC vesicles and at 0–42 mol% in lipid vesicles made with total lipid from whole bovine lenses. Cholesterol was added to some POPC vesicles at 50 mol%.

Anisotropic probes. Two fluorescent anisotropic probes from Molecular Probes, Inc. (Eugene, OR), 2-(3-(diphenylhexatrienyl) propanoyl)-1-hexadecanoyl-*sn*-glycero-3-phosphocholine (DPH-PC) and *N*-(7-nitrobenz-2-oxa-1,3-diazol-4-yl)-1,2-dihexadecanoyl-*sn*-glycero-3-phosphoethanolamine (NBD-PE), were used to assess the influence of U18666A on the order of model lipid membranes and lens lipid membranes. The NBD moiety of NBD-PE localizes to the head group region at the polar interface (23), and the DPH moiety of DPH-PC inserts into the acyl chain region of the lipid bilayer (24). Structures of DPH-PC and NBD-PE can be seen in Gidwani, Holowka, and Baird (24). The molecular probes were incorporated into the model lipid membranes or lens lipid membrane vesicles at 1 mol% or less. Anisotropy was measured using an ISS PC1 counting spectrofluorometer (Champaign, IL). NBD-PE was excited at 460 nm and emission measured at 540 nm. DPH-PC was excited at 362 nm and emission measured at 433 nm. Samples were magnetically stirred during measurements, and data were averaged for at least 100 scans. An increase in the anisotropy indicates reduced molecular motion of the probe, thus indicating that the microenvironment of the probe is more rigid or ordered.

Small-angle X-ray diffraction

Preparation of model membrane vesicles. Multilaminar vesicles were prepared from POPC (Avanti Polar Lipids, Inc., Alabaster, AL) and solubilized in chloroform at 25 mg/ml. Lipid vesicles were prepared with cholesterol at 33 mol% in the absence (control) or presence of U18666A at 3.23 mol% (1 mol of U18666A per 30 mol of total lipid). This concentration is just slightly less than that shown to have a maximum ordering effect on lens membrane lipids (see Fig. 6). Components (in organic solvents) were combined in standard glass test tubes and shell dried under nitrogen gas while vortexing. Residual solvent was removed by drying under vacuum for 3–5 h. Samples were resuspended in diffraction buffer (0.5 mM HEPES, 154 mM NaCl, pH 7.3) and vortex mixed for 3 min at ambient temperature to form multibilayer vesicles (25).

Preparation of lens membrane lipid vesicles. Fiber cell plasma membrane was purified from separated cortex and nucleus of adult bovine lenses by the method of Russell, Robison, and Kinoshita (26), and the lipids were Folch extracted as done before (19). Cholesterol was quantitated by gas chromatography (27) and phospholipids by colorimetric assay (28). Calculated cholesterol-to-phospholipid molar ratios (C/P) in the bovine cortex and nucleus fractions were 0.59 (37 mol% cholesterol) and 2.1 (68 mol% cholesterol), respectively. The C/P of whole lens lipid is ~1.2. The nucleus accounts for ~40% of the total lens mass. Lens lipids were fractionated by thin-layer chromatography, and the phospholipids and cholesterol fractions were separately recovered as done before (29). Lens phospholipids and cholesterol, dissolved in organic solvents, were recombined at C/P at or below that measured in native lens membrane. U18666A, in organic solvent, was added to the preparations at 3.23 mol%, and multilaminar membranes were prepared as described above for the model membranes.

Membrane orientation. Model and lens multilaminar vesicles were oriented for X-ray diffraction analysis as previously described (30). Briefly, 250 μg (phospholipid) of membrane samples (in diffraction buffer) was loaded into lucite sedimentation cells, each containing an aluminum foil substrate upon which the final membrane pellets were collected. The membrane vesicles were centrifuged in a Sorvall AH-629 swinging-bucket ultracentrifuge rotor (DuPont) at 35,000 *g* for 60 min at 5°C. After orientation, sample supernatants were aspirated and the aluminum foil substrates, supporting the membrane pellets, were removed from the sedimentation cells and mounted onto curved glass slides. All samples were equilibrated at 37°C and 74% relative humidity for at least 12 h before diffraction analysis (31).

X-ray diffraction analysis. Oriented membrane samples were aligned at grazing incidence with respect to a collimated, monochromatic X-ray beam (CuK_α $\lambda = 1.54$ Å) produced by a Rigaku Rotoflex RU-200 high-brilliance, rotating-anode microfocus generator (Rigaku USA, Danvers, MA). Coherent scattering data were collected on a one-dimensional, position-sensitive electronic detector. This technique allows for precise measurement of the unit cell periodicity, or *d*-space, of the membrane lipid bilayer, which is the distance from the center of one lipid bilayer to the next, including surface hydration. The *d*-space for any given membrane multibilayer is calculated from Bragg's law ($h\lambda = 2\ d \sin\theta$), where h is the diffraction order number, λ is the wavelength of the X-ray radiation (1.54 Å), d is the membrane lipid bilayer unit cell periodicity, and θ is the Bragg angle equal to one-half the angle between the incident beam and the scatter beam. Fourier transformation of the collected X-ray diffraction data provides the time-averaged electron density distribution (distance, Å, vs. electrons/Å^3) associated with the membrane bilayer. Changes in electron density distribution that occur in the presence of U18666A allow for the measurement of its location in the bilayer. For location analyses, each individual diffraction peak was corrected using a linear subtraction routine that averaged background noise. The lamellar intensity functions from the oriented membrane samples were normalized by a factor of $s = \sin\theta/\lambda$, the Lorentz correction, and phases were assigned to each lamellar diffraction peak based on a swelling or hydration analysis, as previously described (32). Additional details of this method are provided in Jacob, Cenedella, and Mason (31).

RESULTS

OSC cataract formation

Feeding weanling rats U18666A at 0.035% (w/w) of the chow induced cataracts in all animals within 34 days (**Fig. 2**). Other OSC inhibitors (Ro48-8071 and Ro61-0842) fed at a higher level also induced cataracts. Cataractous lenses from both U18666A- and Ro48-treated rats possessed sterol-to-phospholipid molar ratios reduced at ~25% compared with those of lenses from age-matched untreated control rats (**Fig. 3**). Although this observation may suggest that OSC cataracts are related to a selective decrease in the sterol content of lens cells, we previously found that the sterol-to-phospholipid molar ratio was similarly reduced (by ~25%) in both clear and opaque lenses of U18666A-treated rats (33). If the U18666A cataract is attributable to inhibiting lens cell growth through restricting the availability of cholesterol, then maintaining cholesterol should prevent this inhibition. We chose cultured BLECs to test this possibility.

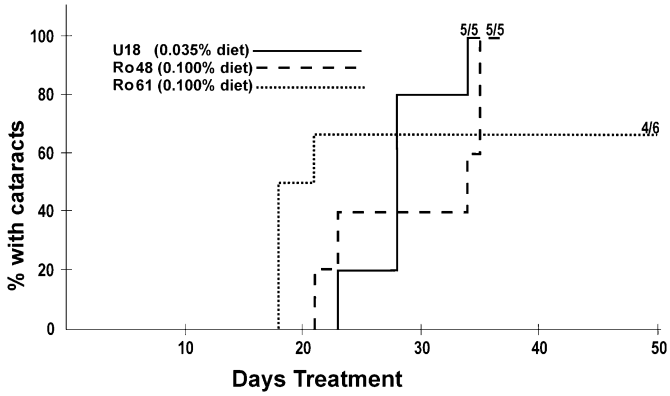

Fig. 2. Induction of cataracts in rats with various OSC inhibitors. Starting at 18–21 days of age, Sprague-Dawley rats were fed ground Purina rat chow containing one of three OSC inhibitors (0.35 or 1.00 g drug/kg chow): U18666A, Ro48-8071 (Ro48), or Ro61-0842 (Ro61).

Effect of U18666A on cultured BLECs

The anterior surface of the lens is covered by a monolayer of epithelial cells, a fraction of which undergo continuous mitosis and terminal differentiation into enormously elongated, largely anucleate fiber cells that form the bulk of the lens mass. This process continues throughout life. Plasma membrane is essentially the only organelle in these cells. Because all cells derive from the epithelial cells and damage of the epithelium is believed to result in various cataracts, such as those related to diabetes and radiation (34), cultured lens epithelial cells constitute a principal model for studying the mechanisms of cataractogenesis (35). The ease with which bovine cells can be established in primary culture make these cells an especially popular model. We assume that the effects of U18666A on these cells mimic the effects of this inhibitor on the intact lens in vivo.

Twenty nanomolar U18666A produced ~40% inhibition of growth of BLECs cultured in cholesterol-deficient culture medium (**Fig. 4**). Complete arrest of net cell growth was seen at between 40 and 50 nM. Although 40 nM U18666A decreased the incorporation of [^{14}C]acetate into BLEC sterols by only 50% (data not shown), the arrest of growth still could be attributable to the restriction of cholesterol availability for plasma membrane formation, because U18666A is known to interfere with the intracellular trafficking of cholesterol (36–38). As the concentration of U18666A was increased, drug levels were reached at which net cell death was evident; i.e., fewer cells present at 48 h (day 3 of culture) than at 0 h (day 1 of culture) (Fig. 4). The mechanism of these reduced cell numbers could be largely independent of cholesterol availability, because cholesterol added back to the medium only slightly antagonized the growth-inhibiting effects of 200 nM U18666A (**Fig. 5**). The inhibiting effects of 30 nM were completely prevented by the presence of cholesterol in the medium. These results suggested that U18666A might exhibit two categories of effects on lens cells, those related to the availability of cholesterol and others independent of cholesterol. The effects seen at the higher levels of drug might be particularly relevant to U18666A's cataractogenic mechanism, because U18666A concentrations as high as 1–2 μM have been measured in whole cataractous lenses of treated rats (39).

Effects of U18666A on the order of lens lipid membranes

The fluorescent anisotropic probe NBD-PE localizes to the head group region, at the interface between the lipid hydrocarbon chains and the polar lipid head groups. DPH-PC inserts into the lipid acyl chain region of the lipid bilayer. The anisotropy data reported by the fluorescent probes are directly related to membrane lipid order: the higher the anisotropic value, the lower the rotational freedom of the probe molecule, indicating an environment that is more ordered or less fluid. In the absence of added U18666A, the anisotropy of DPH-PC in lipid membranes prepared from whole bovine lenses was greater than that of NBD-PE (**Fig. 6**). This is probably attributable to the high cholesterol content in bovine lens membranes, which would be expected to increase the rigidity associated with the hydrocarbon chain region. The lowest concentration of U18666A added to the membranes (4 mol%) induced a marked and nearly maximum increase in the

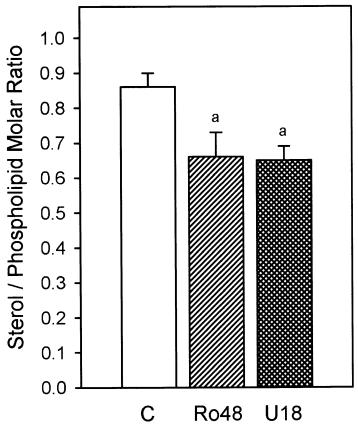

Fig. 3. Effects of treatment with OSC inhibitors on the sterol-to-phospholipid molar ratio in lens total lipids. U18666A and Ro48-8071-treated rats (n = 10 in each group) were killed 2–3 days after the first appearance of cataracts. Lenses from age-matched controls (C; n = 16) were also analyzed. Desmosterol accounted for 37.2 ± 2.8% of total lens sterol in U18666A-treated rats, the rest being cholesterol, and 7.5 ± 1.2% in lenses of Ro48-8071-treated rats. Control lenses possessed 2.4 ± 0.3% desmosterol. Values shown are means ± SEM. [a] Probability by two-tailed *t*-test of the difference from control < 0.01.

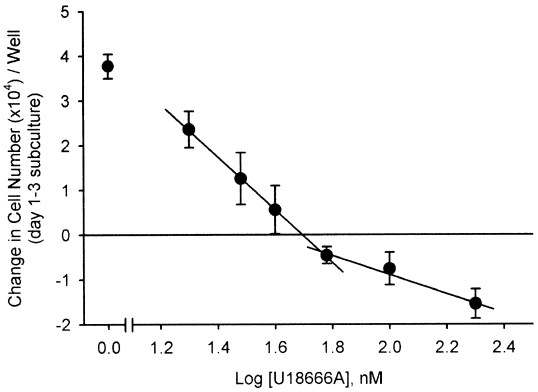

Fig. 4. Effects of U18666A on cell growth/net death of cultured bovine lens epithelial cells (BLECs). Cells seeded at 50,000 were grown in DMEM + 10% lipid-deficient calf serum. Cell numbers were measured after 1 day (time zero) and then grown for an additional 48 h in this medium containing no drug (control) or U18666A. Each point represents the average ± SEM change in cell numbers for three dishes.

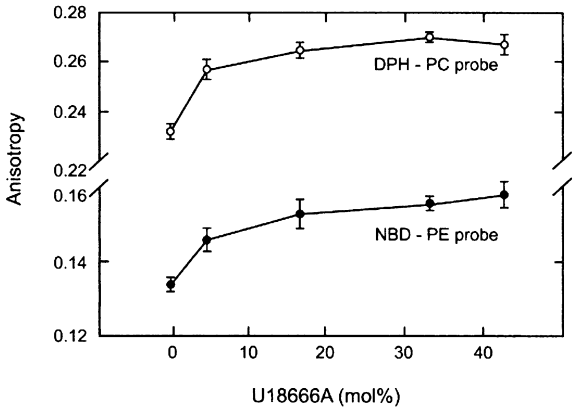

Fig. 6. Dose-response curves of the effect of U18666A on the anisotropy of fluorescent probes incorporated into whole lens lipid membranes (phospholipid plus cholesterol). 2-(3-(Diphenylhexatrienyl)propanoyl)-1-hexadecanoyl-*sn*-glycero-3-phosphocholine (DPH-PC) localizes in the hydrocarbon core of membranes, and *N*-(7-nitrobenz-2-oxa-1,3-diazol-4-yl)-1,2-dihexadecanoyl-*sn*-glycero-3-phosphoethanolamine (NBD-PE) localizes in the polar head group region of the phospholipids. U18666A was incorporated at 0–42 mol% into model membranes prepared from the total lipid recovered from whole bovine lenses. Probes were present at 1 mol%. U18666A at low concentrations increased the anisotropy of both probes, indicating a broad condensing (ordering) effect of the drug on lens membrane structure. Error bars are SEM.

anisotropy of both probes. The anisotropic values associated with the two probes increased only slightly with higher drug levels. These findings indicate that U18666A has a broad condensing effect on membrane lipids, which results in increased membrane order or rigidity. The effects of U18666A (at 2.9 mol%) on the anisotropy of model phospholipid membranes containing cholesterol were similar. The drug's presence increased the anisotropy of NBD-PE as it did in the lens lipid membrane (**Table 1**).

Interaction of U18666A with model membranes

The structural interaction of U18666A with biological membranes was measured using small-angle X-ray diffraction approaches. A representative diffraction pattern, obtained from oriented POPC model membranes prepared in the presence of U18666A (3.2 mol%), is shown in **Fig. 7**. X-ray scattering from this sample yielded reproducible diffraction orders at 20°C; scattering analysis of membranes prepared in the absence of U18666A (control) yielded qualitatively similar diffraction patterns. The unit periodicity, or *d*-space, calculated for control membranes was 58.8 ± 0.3 Å. In the presence of U18666A at 3.2 mol%, the membrane bilayer *d*-space value was relatively unchanged at 58.1 ± 0.3 Å.

One-dimensional electron density profiles, indicating centrosymmetric bilayer structure, were generated from the diffraction data collected from control and U18666A-treated POPC model membrane samples (**Fig. 8**). The two maxima of electron density on either side of the profile correspond to the electron-dense phospholipid head groups, whereas the minimum of electron density at the center of the profile corresponds to the phospholipid ter-

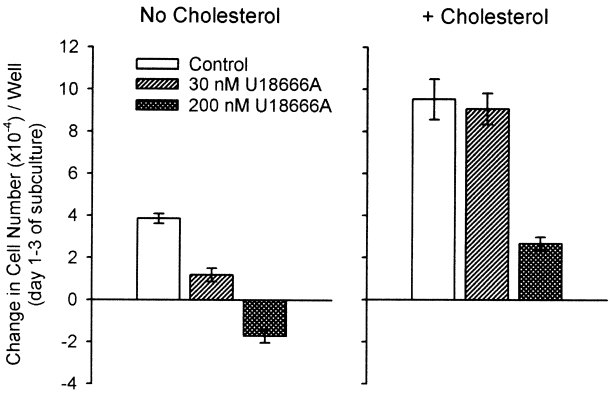

Fig. 5. Effect of cholesterol on growth inhibition of BLECs by "lower" and "higher" levels of U18666A. BLECs were cultured in the presence of 0, 30, or 200 nM U18666A and in the absence (no cholesterol) or presence (+ cholesterol) of cholesterol in the medium. Each point represents the mean ± SEM of six experiments (three dishes of cells per each concentration in each experiments). Cholesterol-containing medium possessed 10% whole calf serum (WCS) plus 50 μg/ml added cholesterol. Cholesterol-free medium possessed 10% delipidated calf serum.

TABLE 1. Cholesterol and U18666A effects on model membrane order

Sample	Head Group-Sensitive Probe NBD-PE Anisotropy (Immobility)
POPC	0.179 ± 0.011
POPC/cholesterol, 1:0.5 (mol/mol)	0.208 ± 0.042
POPC/U18666A, 1:0.03 (mol/mol)	0.255 ± 0.025
POPC/cholesterol/U18666A, 1:0.5:0.03 (mol/mol/mol)	0.248 ± 0.032

Values shown are averages ± SD, n = 3. NBD-PE, *N*-(7-nitrobenz-2-oxa-1,3-diazol-4-yl)-1,2-dihexadecanoyl-*sn*-glycero-3-phosphoethanolamine; POPC, 1-palmitoyl-2-oleoyl-*sn*-glycerol-3-phosphotidylcholine.

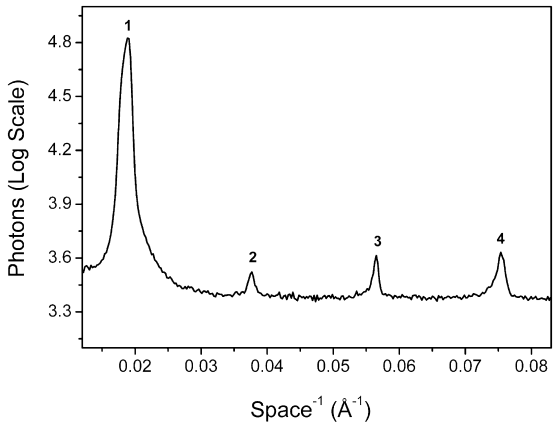

Fig. 7. Representative X-ray diffraction pattern obtained from oriented 1-palmitoyl-2-oleoyl-*sn*-glycerol-3-phosphotidylcholine (POPC) membrane samples containing U18666A at 3.2 mol%. Data were collected on a position-sensitive electronic detector at 20°C and 74% relative humidity. Four diffraction orders were obtained from these membranes, as indicated by the numbers above each peak.

minal methyl segments associated with the center of the membrane bilayer. The effects of U18666A on membrane structure were determined by subtracting the superimposed electron density profiles, as shown in Fig. 8. U18666A treatment resulted in a discrete increase in electron density (±0–10 Å) from the center of the membrane bilayer, consistent with the time-averaged location of the drug.

Interaction of U18666A with bovine lens membranes

We also examined the structural effects of U18666A on fiber cell membranes prepared with phospholipids isolated from bovine lens cortex and nucleus (**Fig. 9**).

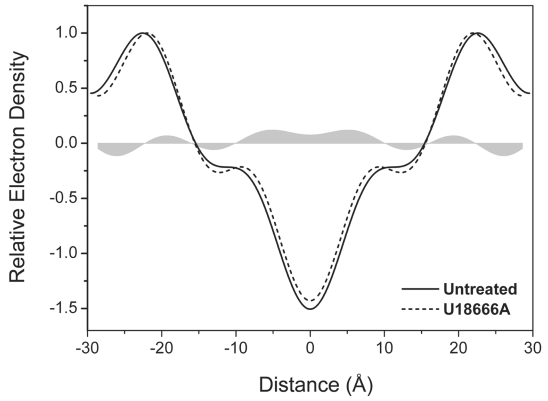

Fig. 8. Superimposed one-dimensional electron density profiles for centrosymmetric POPC membrane bilayers in the absence or presence of U18666A at 3.2 mol%. The maxima of electron density on either side of the profiles correspond to the electron-dense phospholipid head groups, whereas the minimum of electron density at the center of the profile corresponds to the terminal methyl segments associated with the hydrocarbon core of the membrane bilayer. The shaded region indicates the positive difference between the control and drug-treated samples attributable to the presence of U18666A (±0–10 Å from the bilayer center).

U18666A added at 3.2 mol% produced a broad increase in the electron density associated with the hydrocarbon core region in both nuclear (Fig. 9B) and cortical (Fig. 9A) membrane bilayers. Changes along the *x* axis of the electron density profile of ±0.3 Å are considered significant. An increase in electron density of ±9–11 Å from the bilayer center was observed in cortical lens lipid membranes after treatment with U18666A. In nuclear membrane samples, U18666A effected an increase in electron density (±6 Å) from the bilayer center; drug treatment also caused a decrease in intrabilayer width of ±3 Å, which suggests that U18666A alters membrane lipid packing constraints by its interaction with the bilayer. These observations are consistent with the time-averaged location of U18666A in the hydrocarbon core region of both cortical and nuclear bovine lens membranes. It is interesting that the membrane concentration (3.2 mol%) of U18666A that produced this condensing effect on lens membranes is very similar to the concentration (4 mol%) that produced a nearly maximum ordering effect on lens membrane lipids (Fig. 6).

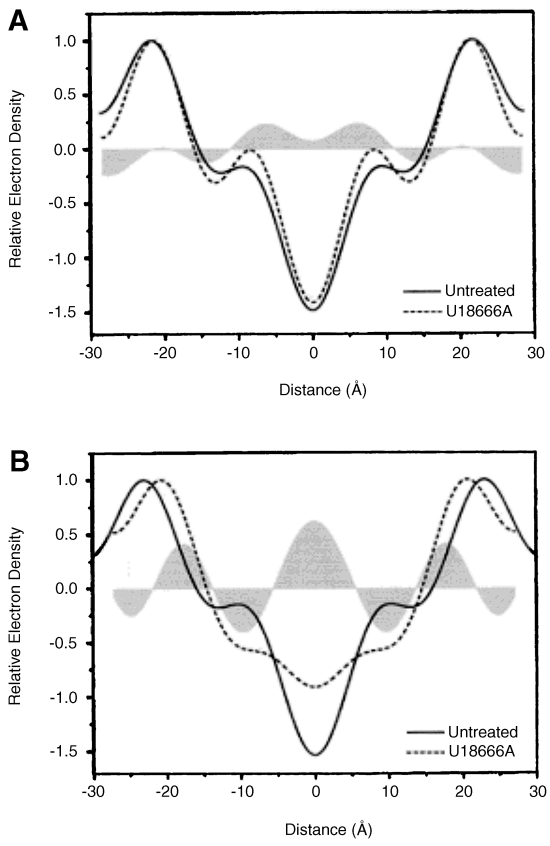

Fig. 9. Distribution of U18666A in bovine lens membranes. A: U18666A produced an increase in electron density (±9–11 Å) from the bilayer center in cortical lens membranes. B: In nuclear lens membrane, U18666A effected an increase in electron density (±6 Å) from the bilayer center and also caused a decrease of ±3 Å in the intrabilayer width (the distance separating the two maxima of electron density). Both cortical and nuclear membrane samples were analyzed at 37°C and 74% relative humidity and contained cholesterol at 37.5 mol%. U18666A was present at 3.2 mol%.

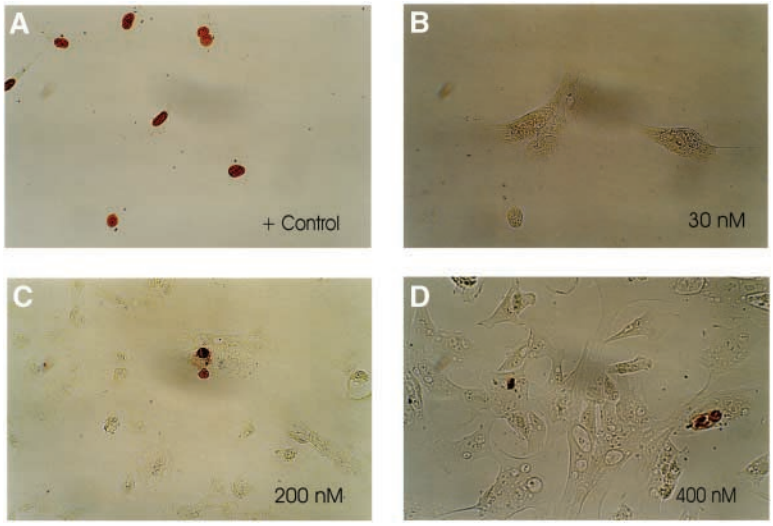

Fig. 10. Induction of apoptosis in cultured BLECs by U18666A. BLECs were cultured in 10% WCS containing 30 nM (B), 200 nM (C), or 400 nM (D) U18666A and evaluated for the presence of apoptotic cells using the DeadEnd apoptosis kit (Promega). Panels show cells after a 48 h exposure. The nuclei of apoptotic cells contain labeled DNA fragments that react with the chromagen and appear brown. A positive control (A) consisted of a cell layer exposed to DNase I to induce DNA fragmentation.

The interaction of U18666A with model membranes (Fig. 8) was examined in several independent experiments and was found to be highly reproducible over a broad range of conditions. U18666A effects in bovine lens membranes (Fig. 9) were also consistent under various temperature and relative humidity conditions.

Induction of apoptosis in lens epithelial cells by U18666A

Culture of BLECs with U18666A in the presence of WCS induced apoptosis (**Fig. 10C**). Apoptosis was also induced in vitro in epithelial cells of the intact lens after 48 h of culture in the presence of 200 nM U18666A (**Fig. 11C**) and after treatment in vivo of rats for 4 weeks with U18666A at 0.035% of the diet (Fig. 11D). Apoptotic epithelial cells were also seen after 3 weeks, but not 2 weeks, of treatment (data not shown). Apoptotic cells were obvious after 2 days of culture of BLECs with 200 nM but not 30 nM U18666A (Fig. 10C, B). A higher drug level (400 nM) induced gross morphological changes characterized by the appearance of many internal vacuoles and lentoid structures (Fig. 10D). Exposure of mouse macrophages to U18666A for 48 h produced similar changes, although higher drug levels were required to produce equivalent effects. One micromolar induced apoptosis and 5 μM decreased cell density and caused cell enlargement, vacuolization, and leakage of cytoplasm (data not shown). The concentration of U18666A in the plasma membrane of these affected cells is unknown and might be much less than the intramembrane levels shown to alter lens lipid membrane order.

DISCUSSION

U18666A could induce cataracts by restricting the availability of cholesterol for the formation of the cholesterol-rich fiber cell plasma membrane, by causing the accumulation of potentially toxic metabolic precursors of cholesterol, or by producing direct, cholesterol-independent effects such as drug intercalation into lens membranes with subsequent disruption of membrane structure and function. Our early hypothesis on the mechanism of

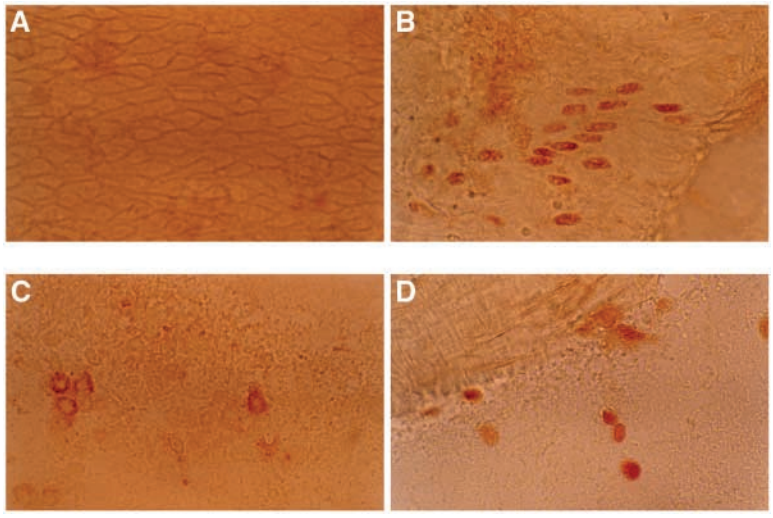

Fig. 11. Induction of apoptosis in rat lenses in vitro and in vivo. Lenses from 20 day old Sprague Dawley rats were cultured for 24 h in TC199 medium containing 0–200 nM U18666A (in vitro) or 20 day old rats were fed U18666A at 0.035% of diet for 28 days (in vivo). Capsules were dissected from the lenses, mounted on glass slides, and stained for apoptotic cells using the DeadEnd apoptosis kit. A: Negative control. B: Positive control (control lenses exposed in vitro to DNase I to induce DNA fragmentation). C: In vitro exposure to U18666A. D: In vivo exposure to U18666A.

the U18666A cataract was simply that by inhibiting lens cholesterol biosynthesis, U18666A decreased the availability of cholesterol for membrane formation (7, 39), which led to damage of the fiber cell membrane (40). Previous studies (33) and the results of the current study show that the development of cataracts in young U18666A-treated rats was accompanied by an ~25% decrease in the molar ratio of cholesterol to phospholipid in lens. Although it is well established that U18666A can decrease cholesterol availability by inhibiting OSC (41) and desmosterol reductase (12), more recent reports indicate that U18666A also inhibits synthesis at sterol Δ8,Δ7-isomerase (42) and the Δ24-isomerase of several intermediates (43). In addition to inhibiting cholesterol synthesis, U18666A is now known to impair intracellular cholesterol trafficking, at minimum, by interfering with the movement of lysosomal cholesterol (derived from extracellular lipoproteins) to the plasma membrane (36) and the movement of cholesterol from the plasma membrane to the endoplasmic reticulum (38).

Several lines of evidence suggest that restricting the availability of cholesterol for the formation of lens cell plasma membrane cannot totally account for U18666A's mechanism of cataractogenesis. The modest reduction in the relative sterol content of lens membrane may be insufficient to result in the gross disorganization of lens membrane structure typical of this cataract (44), particularly when a similar reduction in the sterol-to-phospholipid molar ratio was seen in lenses of U18666A-treated rats that were still clear (33). In the absence of cholesterol in culture medium, BLECs satisfy their sterol requirement by de novo synthesis (21). Inhibition of synthesis inhibits growth. Although cholesterol added to the culture medium reversed the inhibitory effects of a low concentration (30 nM) of U18666A on the growth of BLECs, the inhibition seen at a higher level (200 nM) was only partially antagonized by added cholesterol (Fig. 5). This suggests that U18666A has toxic effects on lens cells independent of restricting cholesterol. The possibility that the formation of toxic metabolites upstream of the inhibited OSC contributes to cataract formation remains to be critically evaluated.

We considered in some detail another possible mechanism of the U18666A cataract, direct intercalation of U18666A into the membrane bilayer with consequent alteration of membrane structure. The structure of U18666A is similar to that of cholesterol except that the iso-octyl group at carbon 17 is replaced by a carbonyl group and the 3β-hydroxyl group at carbon 3 is replaced with a cationic-diethyl amino-ethyl ether (**Fig. 12**). Like cholesterol, U18666A would be expected to migrate to the interface and hydrocarbon chain regions of lipid bilayers. The 3β-hydroxyl group of cholesterol is involved with hydrogen bonding to the sphingolipid amide or glycerolipid carbonyl groups. Instead of the hydroxyl group, the bulky ether group of U18666A would be expected to extend into the head group regions of the bilayer, sterically disrupting the positive lipid-lipid interactions and water bridge network that is present in lipid bilayers. Our spectroscopic data indicate that, as predicted, U18666A spans the head group interface and hydrocarbon chain regions of the bilayer. The drug at ~4 mol% decreased the mobility of the head group-sensitive probe NBD-PE in bovine lens lipids (Fig. 6). Head group probe mobility is also decreased at 2.9 mol% U18666A in POPC and POPC/cholesterol vesicles (Table 1). Fourier transformation analysis of the X-ray scatter data (Fig. 9) indicates that U18666A intercalates into the hydrocarbon core, and in the nuclear membrane it causes an inward shift of the head groups. The spectroscopic data also indicate that, as predicted, U18666A penetrates the hydrocarbon chains. Like cholesterol, U18666A was found to decrease the mobility of the hydrocarbon chain-sensitive probe DPH-PC in bovine lens lipid membranes (Fig. 6). This supports the X-ray scatter data, which showed that the presence of a similar membrane concentration of U18666A resulted in a broad condensing effect on membrane order. We suggest that these U18666A-induced changes in lens membrane structure may contribute to cataract development. Perturbation of membrane structure has also been proposed to contribute to the anticancer activity of tamoxifen (44). Tamoxifen, like U18666A, is a highly lipophilic-amphipathic-ethoxy tertiary amine. Tamoxifen increases the risk of cataracts in treated patients (45, 46).

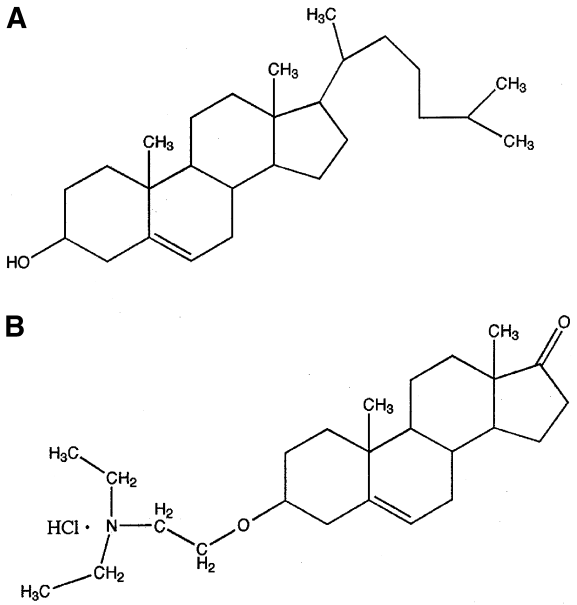

Fig. 12. Comparison of the structure of cholesterol (A) and U18666A (B) [3β-(2-diethylaminoethoxy)-androst-5-en-17one hydrochloride].

U18666A added to lipid membranes at 3–4 mol% both ordered membrane lipids (Table 1, Fig. 6) and condensed the bilayer (Figs. 9, 10). It is difficult to extrapolate this concentration of U18666A in the test lipid membranes to that achieved in lens membranes of U18666A-treated rats. The test concentration could be less, similar, or greater. U18666A was estimated earlier to be present at 2–3 μM in whole lenses of treated rats (39). However, this whole lens concentration most likely greatly underestimates the con-

centration of drug achieved in lens membranes, because U18666A concentrates in lipid-rich membranes (47) and membrane lipids occupy only ~0.6% of the total mass of the rat lens (33). Furthermore, the regional distribution of U18666A in the lens is unknown; it might be restricted to the epithelium and superficial cortex, which occupy less than 10% of the lens's total volume. Also, U18666A might localize in or be excluded from selected membrane domains, such as lipid rafts, or the cholesterol bilayer domain, which we recently identified in lens membranes (31).

We speculate that the membrane lipid-ordering effect of U18666A may alter the activities of lens membranes in vivo. There is support for the capacity of lipid-soluble drugs to rapidly intercalate into biological membranes and alter their physical properties and functions. For example, cortisol added to red blood cells rapidly intercalated into the polar head group region of membrane phospholipids and decreased Na^+/K^+-ATPase activity by 24% (48). Hydrocarbon chain ordering has also been shown to influence the function of lens membranes by decreasing the activity of the Ca-ATPase pumps (49). We have shown that ordered membranes scatter twice as much light as disordered membranes (50). Because U18666A ordered membrane lipids, it could be expected to cause a direct increase of light scatter.

Whether by changing membrane structure or through more specific actions, induction of apoptosis by U18666A in lens epithelial cells could be important to cataract development. An intact epithelial cell layer is essential for maintaining water and nutrient flux into and out of the lens body and for the sustained growth of the lens through continuous differentiation of epithelial cells into fiber cells (35). Loss of lens epithelial cells through apoptosis appears to be a common feature of various experimental cataracts (34, 51). The role of apoptosis in the development of human senile cataracts is controversial (51, 52).

The observed capacity of U18666A to induce apoptosis and disrupt the structure of both cultured lens epithelial cells and macrophages appears to conflict with the findings of Kellner-Weibel, Geng, and Rothblat (53) that micromolar levels of U18666A protected lipid-laden J774 macrophages from apoptosis associated with the inhibition of acyl coenzyme-A:cholesterol acyltransferase. Twenty-four hours of exposure of the macrophages to U18666A prevented the transport of toxic free cholesterol to the cell's plasma membrane (53). The stark contrast between our findings and theirs could be that they used lipid-engorged cells. Growing macrophages in the presence of modified LDL can result is massive lipid accumulation (54). Our cells were not lipid laden. Because U18666A appears to concentrate in lipid-rich subcellular structures (47), U18666A may largely partition into macrophage lipids, thereby decreasing the drug's toxicity. Adequate drug levels may remain in the cytosol to inhibit cholesterol trafficking.

In conclusion, U18666A appears to have a profound effect on lens cells that could be largely independent of restricting the availability of cholesterol for lens membrane growth. The capacity of U18666A to intercalate into lens lipid membranes and alter their physical properties could contribute to cataract formation by both inducing apoptosis of lens epithelial cells and causing membranes to scatter more light. It is also possible that the U18666A-induced apoptosis could be independent of changing lens membrane structure. For example, Smets, Van Rooij, and Salomons (55) observed that apoptosis induced in mouse lymphoma cells by a specific ether lipid was attributable to stress mediated by reactive oxygen species rather than to changing membrane physical properties.

The authors thank Dr. Olivier Morand (Roche Pharmaceuticals, Basel, Switzerland) for samples of Ro48-8071 and Ro61-0842. This research was supported by National Institutes of Health Grants EY-02568 to R.J.C. and EY-07975 to D.B.

REFERENCES

1. Cenedella, R. J. 1996. Cholesterol and cataracts. *Surv. Ophthalmol.* **40:** 320–337.
2. Hoffmann, G., K. M. Gibson, I. K. Brandt, P. I. Bader, R. S. Wappener, and L. Sweetman. 1986. Mevalonic aciduria—an inborn error of cholesterol and nonsterol isoprene biosynthesis. *N. Engl. J. Med.* **314:** 1610–1614.
3. Derry, J. M., E. Gormally, G. D. Means, W. Zhao, A. Meindl, R. I. Kelley, Y. Boyd, and G. E. Herman. 1999. Mutations in a delta 8-delta 7 sterol isomerase in the tattered mouse and X-linked dominant chondrodysplasia punctata. *Nat. Genet.* **22:** 286–290.
4. Tint, G. S., M. Irons, E. R. Elias, A. K. Batta, R. Frieden, T. S. Chen, and G. Salen. 1994. Defective cholesterol biosynthesis associated with the Smith-Lemli-Opitz syndrome. *N. Engl. J. Med.* **330:** 107–113.
5. FitzPatrick, D. R., J. W. Keeling, M. J. Evans, A. E. Kan, J. E. Bell, M. E. Porteous, K. Mills, R. M. Winter, and P. T. Clayton. 1998. Clinical phenotype of desmosterolosis. *Am. J. Med. Genet.* **75:** 145–152.
6. von Sallmann, L. 1963. Triparanol-induced cataracts in rats. *Trans. Am. Ophthalmol. Soc.* **61:** 49–60.
7. Cenedella, R. J., and G. G. Bierkamper. 1979. Mechanism of cataract production by 3-beta(2-diethylaminoethoxy)androst-5-en-17-one hydrochloride, U18666A: an inhibitor of cholesterol biosynthesis. *Exp. Eye Res.* **28:** 673–688.
8. Pyrah, I. T., A. Kalinowski, D. Jackson, W. Davies, S. Davis, A. Aldridge, and P. Greaves. 2001. Toxicologic lesions associated with two related inhibitors of oxidosqualene cyclase in the dog and mouse. *Toxicol. Pathol.* **29:** 174–179.
9. Cenedella, R. J., J. R. Kuszak, K. J. Al-Ghoul, S. Qin, and P. S. Sexton. 2003. Discordant expression of the sterol pathway in lens underlies simvastatin-induced cataracts in Chbb:Thom rats. *J. Lipid Res.* **44:** 198–211.
10. Schlienger, R. G., W. E. Haefeli, H. Jick, and C. R. Meier. 2001. Risk of cataract in patients treated with statins. *Arch. Intern. Med.* **161:** 2021–2026.
11. Kantola, T., K. T. Kivisto, and P. J. Neuvonen. 1998. Erythromycin and verapamil considerably increase serum simvastatin and simvastatin acid concentrations. *Clin. Pharmacol. Ther.* **64:** 177–182.
12. Phillips, W. A., and J. Avigan. 1963. Inhibition of cholesterol biosynthesis in the rat by 3 beta-(2-diethylaminoethoxy)androst-5-en-17-one hydrochloride. *Proc. Soc. Exp. Biol. Med.* **112:** 233–236.
13. Mark, M., P. Muller, R. Maier, and B. Eisel. 1996. Effects of a novel 2,3-oxidosqualene cyclase inhibitor on the regulation of cholesterol biosynthesis in HepG2 cells. *J. Lipid Res.* **37:** 148–158.
14. Eisele, B., R. Budzinski, P. Muller, R. Maier, and M. Mark. 1997. Effects of a novel 2,3-oxidosqualene cyclase inhibitor on cholesterol biosynthesis and lipid metabolism in vivo. *J. Lipid Res.* **38:** 564–575.
15. Morand, O. H., J. D. Aebi, H. Dehmlow, Y. H. Ji, N. Gains, H. Lengsfeld, and J. Himber. 1997. Ro 48-8.071, a new 2,3-oxidosqualene:lanosterol cyclase inhibitor lowering plasma cholesterol in hamsters, squirrel monkeys, and minipigs: comparison to simvastatin. *J. Lipid Res.* **38:** 373–390.

16. Isaac, N. E., A. M. Walker, H. Jick, and M. Gorman. 1991. Exposure to phenothiazine drugs and risk of cataract. *Arch. Ophthalmol.* **109:** 256–260.
17. Herbette, L., C. A. Napolitano, F. C. Messineo, and A. M. Katz. 1985. Interaction of amphiphilic molecules with biological membranes. A model for nonspecific and specific drug effects with membranes. *Adv. Myocardiol.* **5:** 333–346.
18. Golden, G. A., P. E. Mason, R. T. Rubin, and R. P. Mason. 1998. Biophysical membrane interactions of steroid hormones: a potential complementary mechanism of steroid action. *Clin. Neuropharmacol.* **21:** 181–189.
19. Fleschner, C. R., and R. J. Cenedella. 1991. Lipid composition of lens plasma membrane fractions enriched in fiber junctions. *J. Lipid Res.* **32:** 45–53.
20. Rothblat, G. H., L. Y. Arbogast, L. Ouellette, and B. V. Howard. 1976. Preparation of delipidized serum protein for use in cell culture systems. *In Vitro.* **12:** 554–557.
21. Hitchener, W. R., and R. J. Cenedella. 1985. Absolute rates of sterol synthesis estimated from [^{3}H]water for bovine lens epithelial cells in culture. *J. Lipid Res.* **26:** 1455–1463.
22. Byrdwell, W. C., H. Sato, A. Schwarz, M. C. Yappert, D. Borchman, and D. Tang. 2002. ^{31}P NMR quantification and monophasic solvent purification of human and bovine lens phospholipids. *Lipids.* **37:** 1087–1092.
23. Chattopadhyay, A., and E. London. 1987. Parallax method for direct measurement of membrane penetration depth utilizing fluorescence quenching by spin-labeled phospholipids. *Biochemistry.* **26:** 39–45.
24. Gidwani, A., D. Holowka, and B. Baird. 2001. Fluorescence anisotropy measurements of lipid order in plasma membranes and lipid rafts from RBL-2H3 mast cells. *Biochemistry.* **40:** 12422–12429.
25. Bangham, A. D., M. M. Standish, and J. C. Watkins. 1965. Diffusion of univalent ions across the lamellae of swollen phospholipids. *J. Mol. Biol.* **13:** 238–252.
26. Russell, P., W. G. Robison, Jr., and J. H. Kinoshita. 1981. A new method for rapid isolation of the intrinsic membrane proteins from lens. *Exp. Eye Res.* **32:** 511–516.
27. Cenedella, R. J. 1982. Digitonide precipitable sterols: a reevaluation with special attention to lanosterol. *Lipids.* **17:** 443–447.
28. Pollet, S., S. Ermidou, F. Le Saux, M. Monge, and N. Baumann. 1978. Microanalysis of brain lipids: multiple two-dimensional thin-layer chromatography. *J. Lipid Res.* **19:** 916–921.
29. Borchman, D., R. J. Cenedella, and O. P. Lamba. 1996. Role of cholesterol in the structural order of lens membrane lipids. *Exp. Eye Res.* **62:** 191–197.
30. Mason, R. P., W. J. Shoemaker, L. Shajenko, T. E. Chamers, and L. G. Herbette. 1992. Evidence for changes in the Alzheimer's disease brain cortical membrane structure mediated by cholesterol. *Neurobiol. Aging.* **13:** 413–419.
31. Jacob, R. F., R. J. Cenedella, and R. P. Mason. 1999. Direct evidence for immiscible cholesterol domains in human ocular lens fiber cell plasma membranes. *J. Biol. Chem.* **274:** 31613–31618.
32. Moody, M. F. 1963. X-ray diffraction pattern of nerve myelin: a method for determining the phases. *Science.* **142:** 1173–1174.
33. Cenedella, R. J. 1985. Regional distribution of lipids and phospholipase A2 activity in normal and cataractous rat lens. *Curr. Eye Res.* **4:** 113–120.
34. Takamura, Y., E. Kubo, S. Tsuzuki, and Y. Akagi. 2003. Apoptotic cell death in the lens epithelium of rat sugar cataracts. *Exp. Eye Res.* **77:** 51–57.
35. Bhat, S. P. 2001. The ocular lens epithelium. *Biosci. Rep.* **21:** 537–563.
36. Liscum, L., and J. R. Faust. 1989. The intracellular transport of low density lipoprotein derived cholesterol is inhibited in Chinese hamster ovary cells cultured with 3-beta-[2-(diethylamino)ethoxy]androst-5-en-17-one. *J. Biol. Chem.* **264:** 11796–11806.
37. Liscum, L., and K. W. Underwood. 1995. Intracellular cholesterol transport and compartmentation. *J. Biol. Chem.* **270:** 15443–15446.
38. Feng, B., and I. Tabas. 2002. ABCA1-mediated cholesterol efflux is defective in free cholesterol-loaded macrophages. Mechanism involves enhanced ABCA1 degradation in a process requiring full NPC1 activity. *J. Biol. Chem.* **277:** 43271–43280.
39. Cenedella, R. J. 1983. Source of cholesterol for the ocular lens, studied with U18666A: a cataract-producing inhibitor of lipid metabolism. *Exp. Eye Res.* **37:** 33–43.
40. Kuszak, J. R., A. R. Khan, and R. J. Cenedella. 1988. An ultrastructural analysis of plasma membrane in the U18666A cataract. *Invest. Ophthalmol. Vis. Sci.* **29:** 261–267.
41. Panini, S. R., R. C. Sexton, and H. Rudney. 1984. Regulation of 3-hydroxy-3-methylglutaryl coenzyme A reductase by oxysterol byproducts of cholesterol biosynthesis. Possible mediators of low density lipoprotein action. *J. Biol. Chem.* **259:** 7767–7771.
42. Moebius, F. F., R. J. Reiter, K. Bermoser, H. Glossmann, S. Y. Cho, and Y. K. Paik. 1998. Pharmacological analysis of sterol delta8-delta7 isomerase proteins with [^{3}H]ifenprodil. *Mol. Pharmacol.* **54:** 591–598.
43. Bae, S. H., and Y. K. Paik. 1997. Cholesterol biosynthesis from lanosterol: development of a novel assay method and characterization of rat liver microsomal lanosterol delta 24-reductase. *Biochem. J.* **326:** 609–616.
44. Engelk, M., P. Bojarski, R. Bloss, and H. Diehl. 2001. Tamoxifen perturbs lipid bilayer order and permeability: comparison of DSC, fluorescence anisotropy, laurdan generalized polarization and carboxyfluorescein leakage studies. *Biophys. Chem.* **90:** 157–173.
45. AstraZeneca. 2002. Novadex. *In* Physician's Desk Reference. Medical Economics Company, Montvale, NJ. Vol. 56. 678–684.
46. Gorin, M. B., R. Day, J. P. Constantino, B. Fisher, C. K. Redmond, L. Wickerham, J. E. Gomolin, R. G. Margolese, M. K. Mathen, D. M. Bowman, D. I. Kaufman, N. V. Dimitrov, L. J. Singerman, R. Bornstein, N. Wolmark, and D. Kaufmann. 1998. Long-term tamoxifen citrate use and potential ocular toxicity. *Am. J. Ophthalmol.* **125:** 493–501.
47. Cenedella, R. J., C. P. Sarkar, and L. Towns. 1982. Studies on the mechanism of the epileptiform activity induced by U18666A. II. Concentration, half-life and distribution of radiolabeled U18666A in the brain. *Epilepsia.* **23:** 257–268.
48. Golden, G. A., R. P. Mason, T. N. Tulenko, G. S. Zubenko, and R. T. Rubin. 1999. Rapid and opposite effects of cortisol and estradiol on human erythrocyte Na^{+},K^{+}-ATPase activity: relationship to steroid intercalation into the cell membrane. *Life Sci.* **65:** 1247–1255.
49. Zeng, J., Z. Zhang, C. A. Paterson, S. Ferguson-Yankey, M. C. Yappert, and D. Borchman. 1999. Ca(2+)-ATPase activity and lens lipid composition in reconstituted systems. *Exp. Eye Res.* **69:** 323–330.
50. Tang, D., D. Borchman, M. C. Yappert, G. F. Vrensen, and V. Rasi. 2003. Influence of age, diabetes, and cataract on calcium, lipid-calcium, and protein-calcium relationships in human lenses. *Invest. Ophthalmol. Vis. Sci.* **44:** 2059–2066.
51. Li, W. C., J. R. Kuszak, K. Dunn, R. R. Wang, W. Ma, G. M. Wang, A. Spector, M. Leib, A. M. Cotliar, M. Weiss, J. Espy, G. Howard, R. L. Farris, J. Auran, A. Donn, A. Hofeldt, C. Mackay, J. Merriam, R. Mittl, and T. R. Smith. 1995. Lens epithelial cell apoptosis appears to be a common cellular basis for non-congenital cataract development in humans and animals. *J. Cell Biol.* **130:** 169–181.
52. Harocopos, G. J., K. M. Alvares, A. E. Kolker, and D. C. Beebe. 1998. Human age-related cataract and lens epithelial cell death. *Invest. Ophthalmol. Vis. Sci.* **39:** 2696–2706.
53. Kellner-Weibel, G., Y. J. Geng, and G. H. Rothblat. 1999. Cytotoxic cholesterol deposition in macrophages mediated by cholesterol-enriched oxidized low density lipoproteins. *Atherosclerosis.* **146:** 309–319.
54. Greenspan, P., H. Yu, F. Mao, and R. L. Gutman. 1997. Cholesterol deposition in macrophages: foam cell formation mediated by cholesterol-enriched oxidized low density lipoprotein. *J. Lipid Res.* **38:** 101–109.
55. Smets, L. A., H. Van Rooij, and G. S. Salomons. 1999. Signalling steps in apoptosis by ether lipids. *Apoptosis.* **4:** 419–427.